

## Neutral mesons flow and yields in AgAg@1.58 AGeV at HADES

---

**Alexandr Prozorov<sup>a,b,\*</sup> for the HADES collaboration**

<sup>a</sup>*Nuclear Physics Institute, Hlavni 130, Rez, Czech Republic*

<sup>b</sup>*Charles University, Faculty of Mathematics and Physics, Ke Karlovu 3, Praha 2, Czech Republic*

*E-mail: [prozorov@ujf.cas.cz](mailto:prozorov@ujf.cas.cz)*

The Dielectron Spectrometer HADES operated at the SIS18 synchrotron, FAIR/GSI Darmstadt recently provided new intriguing results on production of electron pairs and of strangeness from nucleus-nucleus collisions, as well as from elementary reactions, in energy region of 1 – 2 A GeV. In 2019 the spectrometer was complemented by an electromagnetic calorimeter based on lead-glass modules, which allows us to measure photons and thus to study the production of  $\pi^0$  and  $\eta$  mesons via their two-photon decay. Knowledge of the neutral-meson production is a mandatory prerequisite for the interpretation of dielectron data. In particular, the directed and elliptic flow of neutral mesons will be shown with respect to transverse momentum and rapidity for different centrality classes in Ag + Ag collisions at 1.58 A GeV. The results of the analysis corresponding to the  $14 \times 10^9$  events will be confronted with the results of other experiments and with the current model calculations.

*FAIR next generation scientists - 7th Edition Workshop (FAIRness2022)*

*23-27 May 2022*

*Paralia (Pieria, Greece)*

---

\*Speaker

## 1. Introduction and HADES experiment

Conditions similar to the interior of neutron stars can be accessed in the heavy-ion collisions with high energy. One of the promising observables of the macroscopic properties of the collision are the virtual photons that carry information from inside of the hot and dense matter, which is formed in the collision zone. Furthermore, they do not interact strongly with the medium and allow one to "look into" the early stages of collision. The neutral pion yield is important because its  $e^+e^-$  decay contributes significantly to the yield of  $e^+e^-$  pairs [1].

Further, knowledge of the nuclear Equation-of-State at high densities is essential for our understanding of the nuclear forces as well as for astrophysical purposes. The time evolution of hadronic matter can be described by the laws of hydrodynamics, assuming that thermalization is achieved in the early stages of heavy-ion collisions and that the interaction between the quarks is strong enough to maintain local thermodynamic equilibrium during subsequent expansion. One of the properties of EoS is the incompressibility of nuclear matter, which describes the resistance of matter to compression and is closely related to particle flow. Radial flow characterizes the collision system in kinetic freeze-out, that is, when elastic collisions of the produced particles cease[2].

The HADES setup consists of an ironless six-coil toroidal magnet centered on the beam axis and six identical detector sectors located between the coils. It has acceptance of a nearly complete azimuthal coverage and polar angles that span between  $18^\circ \leq \theta \leq 85^\circ$ . Each sector is equipped with a central hadron-blind RICH detector, four planes of Mini Drift Chambers, a time-of-flight detectors (Resistive Plate Chamber (RPC) and Time-of-Flight Wall), Electromagnetic Calorimeter (ECAL), and Forward Wall (FWALL). Fig. 1 shows a schematic view of the setup. For more references, see [3], [4].

The newly installed Electromagnetic Calorimeter offers a unique possibility for the HADES spectrometer to measure neutral particles. The total area of the HADES calorimeter is approximately  $8 \text{ m}^2$  and covers the polar angles between  $12^\circ$  and  $45^\circ$  with almost full azimuthal coverage. The resolution of the photon and electron energy achieved in the test experiments amounts to  $\approx 6\%/\sqrt{E}$ . The main element of the HADES ECAL is the modified module of the OPAL end cap electromagnetic calorimeter with CEREN 25 lead glass inside that is used as a Cherenkov radiator.

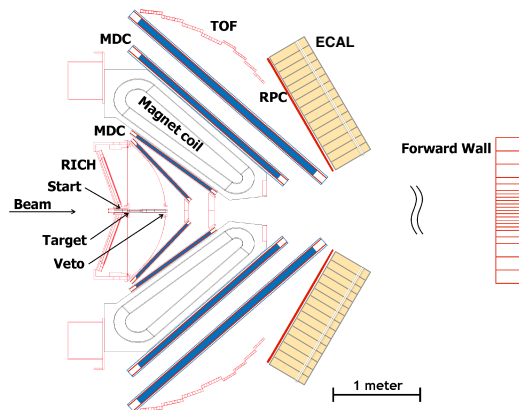


**Figure 1:** A schematic view of a cross section through two opposite sectors of HADES.

## 2. Data analysis and yields

A photon can be reconstructed by demanding a condition of anti-matching with any reconstructed charged track and by the anticoincidence with the RPC detector, which stands in front of ECAL. The detector energy response should be greater than 100 MeV. This energy cut removes most

of the neutrons, which could also interact hadronically with ECAL. In addition to those cuts, the particle velocity condition  $\beta > 0.8$  is applied. The calibration of the ECAL detector was performed in two steps. Firstly, using reconstructed electrons in HADES, one gets a first estimate of the calibration coefficients. Secondly, by several iterations, these coefficients were slightly modified by requiring the  $\pi^0$  peak position equal to the known value of 134,98 MeV.

It is not possible to identify which photons originated from the same meson decay; therefore, all possible combinations of  $\gamma\gamma$  are taken into account within one event ( $All_{\gamma\gamma}$ ). Most combinations contribute to the so-called *combinatorial background* ( $CB_{\gamma\gamma}$ ). To estimate the combinatorial background, the event mixing method was used. This method consists of combining photons originating from different events because those particles are not correlated, and hence the correlated signal is absent, and it can be used for the subtraction from one-event photon combinations. These photon combinations must also have the same event topology, including centrality, photon multiplicity, and vertex position. An example of  $\pi^0$  signal extraction is shown in Fig.2. Efficiency and acceptance corrections are applied, based on GEANT simulations of the HADES setup.

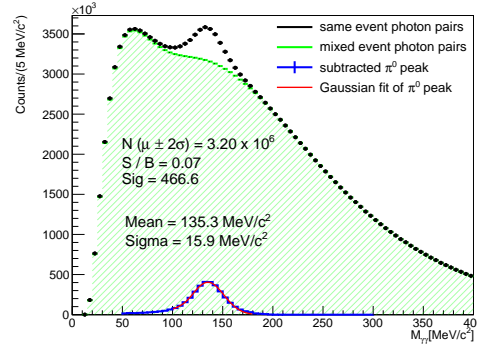


**Figure 2:** An example of  $\pi^0$  number extraction. The black line represents same-event pairs, green points - mixed-event pairs, the blue points represent the correlated signal, and the red line shows the fit of extracted signal.

The comparison of neutral pion yield with an average of  $\pi^+$  and  $\pi^-$  yields in the rapidity distribution can be seen in left Fig. 3. The phase-space distribution of  $\pi^0$  yields with Boltzmann fits  $\frac{dN}{dp_t} = C p_t m_t e^{-\frac{m_t}{T}}$  is shown on the right.

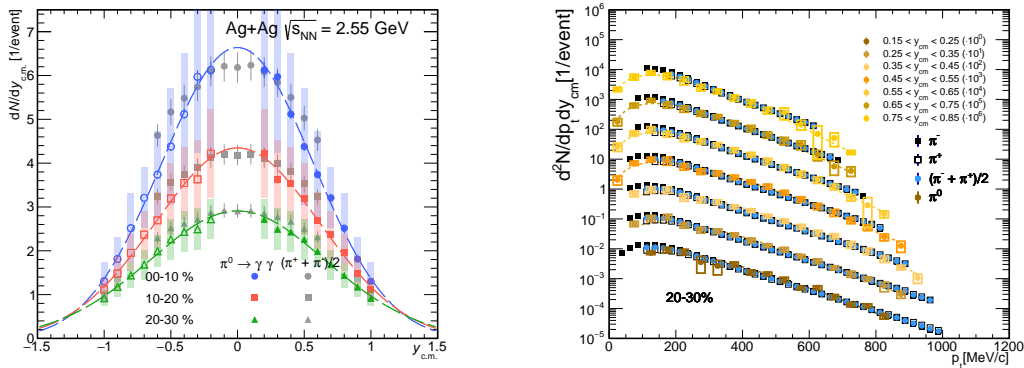


**Figure 3:** **Left:** Comparison with an average of charged pions yields. Error bars represent the systematic uncertainties. **Right:** The pion yield in phase space with Boltzmann fits

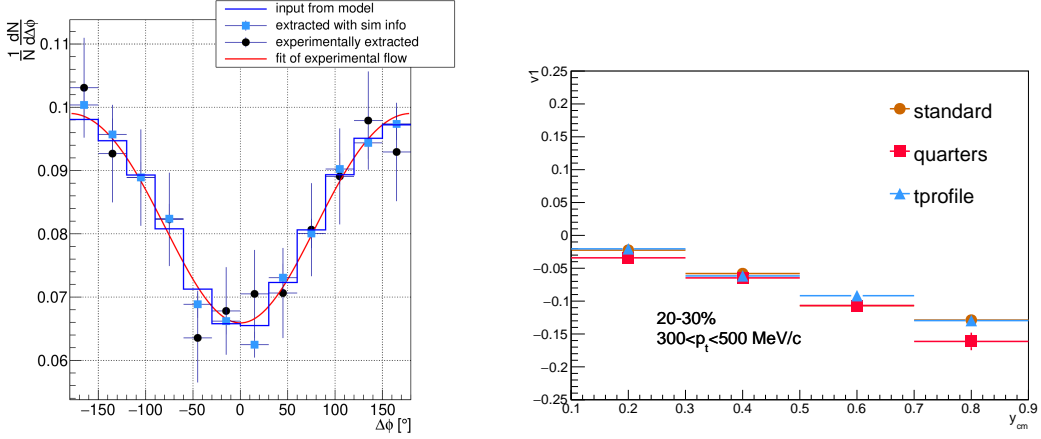


**Figure 4:** **Left:** Simulation check, dark blue histogram shows original UrQMD distribution, light blue is reconstructed flow with additional GEANT info, black point represent the reconstructed flow as in experiment, red line is the fit of black points. **Right:** Comparison of methods for systematics.

### 3. Flow

To characterize the distribution of the particles, an expansion of the angular distribution of the particles relative to the reaction plane into a Fourier series is used [2].

The flow coefficient calculation procedure was first checked in the simulations, as shown in Fig. 4. The original input from the UrQMD model was digitized and then further reconstructed using GEANT simulations.

For the estimation of the reaction plane angle  $\Psi_{EP}$  as well as its resolution correction factors, a dedicated detector FWALL was used. The number of extracted neutral pions  $dN(p_t, y, C)/\Delta\phi$  in different  $\Delta\phi = \phi - \Psi_{EP}$  bins is examined in different phase-space regions in  $p_t$ -  $y$  and in the centrality class  $C$ . This distribution is further fitted with a Fourier decomposition:  $\frac{dN(p_t, y, C)}{\Delta\phi} = \frac{N}{2\pi} (1 + 2v_1^{obs} \cos \Delta\phi + 2v_2^{obs} \cos 2\Delta\phi)$ .

For the systematic uncertainty of the flow coefficients, two more methods were used in addition to the usual standard fitting method, that is, the "quadrant method", which involves the distribution of the azimuthal angle in quarters with respect to the event plane.

$$R_{in-plane} = \frac{N_0}{N_{180}}, \quad R_{squeeze} = \frac{N_{90} + N_{270}}{N_0 + N_{180}},$$

$$v_2^{obs} = \frac{1}{2} \frac{1 - R_{squeeze}}{1 + R_{squeeze}}, \quad v_1^{obs} = \frac{1}{2} \frac{(1 + 2v_2^{obs})(R_{in-plane} - 1)}{1 + R_{in-plane}},$$

where  $N_m$  is the number of reconstructed  $\pi^0$  in the  $90^\circ$  bin around its middle value  $m$ .

The third method uses invariant mass distribution [6].  $N_{cand}(m_{inv}) = N_S(m_{inv}) + N_B(m_{inv})$ . Furthermore, the decomposition of the flow harmonic  $n$  can be done for the observed mean value over all candidates in events.  $v_{n,S+B}^{obs}(m_{\gamma\gamma}) = v_{n,S}^{obs}(m_{\gamma\gamma}) + v_{n,B}^{obs}(m_{\gamma\gamma})$ .

The TProfile histogram is filled with  $\langle \cos[n(\phi - \Psi_1)] \rangle(m_{inv})$  for each diphoton track. The histogram for the invariant mass of two photons is filled in parallel, using both same-event and mixed-event techniques. Then the signal-to-background ratio is calculated based on these usual histograms and then used to fit TProfile to  $v_{n,S}^{obs}(m_{\gamma\gamma})$ .

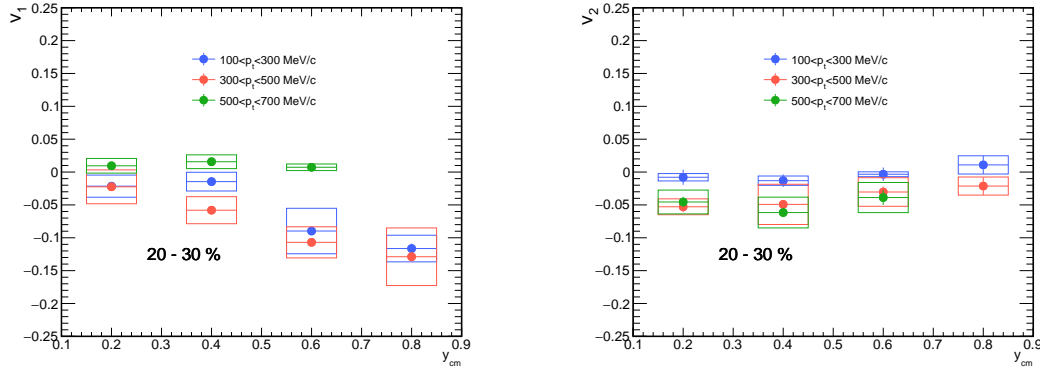


**Figure 5:** Flow of the neutral pions for 20-30 %. **Left:** Directed flow. **Right:** Elliptic flow.

The check of the three methods is shown in Fig. 4. The standard method was used for the results for directed and elliptic flow, and they are shown in Fig. 5, the standard method is used here.

The extracted flow coefficients are further compared with various models, as seen in Fig. 6. In Fig. 7 the UrQMD with EoS model is shown. It has a much better agreement with an experimental data both for directed and elliptic flows of neutral pions, because it was adjusted for the flow of different experimental data in this energy-regime and contains some phenomenological parameters. Based on these figures, the following observations can be made:

- directed flow is dependent on a transverse momentum,
- elliptic flow is approximately constant as a function of rapidity and decreases towards higher transverse momentum,
- neutral pion species show similar behavior as in UrQMD with EoS,
- neutral pion directed flow is stronger in some  $p_t$  bins than that of charged pions, which is not the case for UrQMD with EoS.
- elliptic flow of all three pion species is the same.

#### 4. Conclusion

A newly installed electromagnetic calorimeter was successfully used in the experiment. The calibration of ECAL was performed on the basis of the leptons registered in ECAL and requiring that  $\pi^0$  peak position was at the known value of 134.98 MeV, and the resulting energy resolution was 6%. First results on neutral pion yields at such energies in heavy projectile-target collision system were reported.

#### Acknowledgment

Work supported by: NPI CAS, Rez, Rez (Czech Republic), MSMT LTT17003, MSMT LM2018112, MSMT OP VVV CZ.02.1.01/0.0/0.0/18\_046/0016066

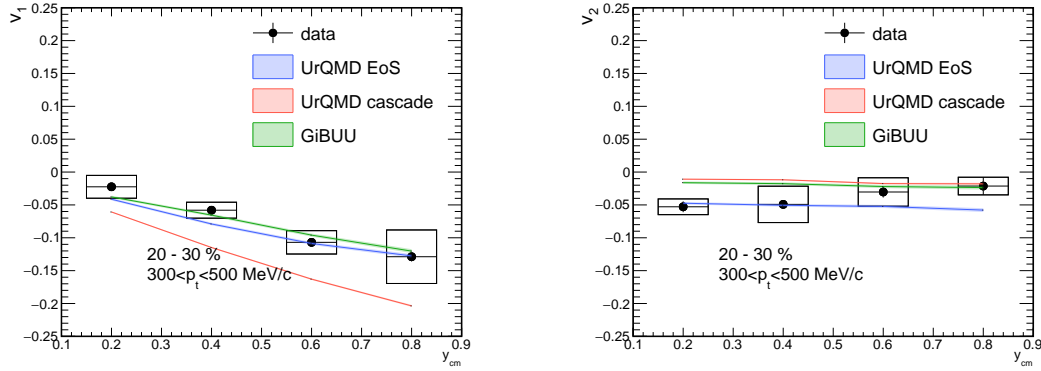


**Figure 6:** Left: Comparison of directed flow model predictions. Right: Comparison of elliptic flow with model predictions.

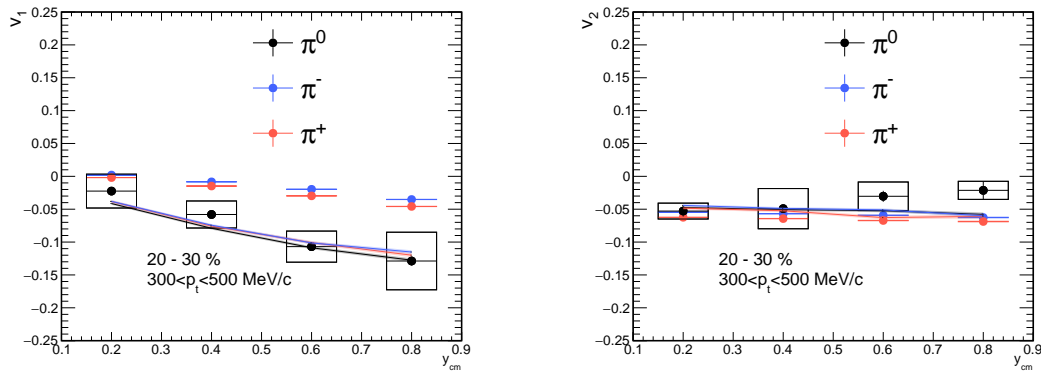


**Figure 7:** Flow of all pions for 20-30% compared with UrQMD EOS. Left: Directed flow. Right: Elliptic flow.

## References

- [1] Tetyana Galatyuk, HADES overview, <https://doi.org/10.1016/j.nuclphysa.2014.10.044>.
- [2] A. M. Poskanzer and S. Voloshin. Methods for analyzing anisotropic flow in relativistic nuclear collisions, 1998, PhysRev.C58 1671
- [3] G. Agakishiev et al. The High-Acceptance Dielectron Spectrometer HADES. Eur. Phys. J. A, 41:243–277, 2009. doi: 10.1140/epja/i2009-10807-5.
- [4] O. Svoboda et al. Electromagnetic calorimeter for the HADES@FAIR experiment, doi:10.1088/1748-0221/9/05/C05002
- [5] G. Agakishiev et al. Dielectron production in Ar + KCl collisions at 1.76A GeV doi: 10.1103/PhysRevC.84.014902
- [6] N. Borghini and J. Y. Ollitrault. Azimuthally sensitive correlations in nucleus-nucleus collisions. Physical Review C 70 (6). 2004